Evaluation of Anti-Cancer, Pro-Apoptotic, and Anti-Metastatic Effects of Synthetic Analogue Compound 2-Imino-7-Methoxy-4-(4-fluorophenyl)-2H-1,3-Thiazino [3,2-a] Benzimidazole on Pancreatic PaCa-2 and Melanoma A375 Cancer Cells

Mpho Ndou[1], Marthe C. D. Fotsing[2], Michael H. K. Kengne[2], Edwin M. Mmutlane[2], Derek T. Ndinteh[2], Mthokozisi B.C. Simelane[1], Lesetja Motadi[1], Mpho S. Choene[1]

[1] *Department of Biochemistry, Faculty of Science, University of Johannesburg, South Africa*
[2] *Department of Chemical Sciences, Faculty of Chemistry, University of Johannesburg, South Africa*

Received: 11 Jan. 2024; Accepted: 11 Sep. 2024

Abstract- Synthetic compounds are widely used in cancer drug discovery. Chemotherapies aim to inhibit proliferation and induce apoptosis however, they have limitations. This study aims to explore in vitro anti-proliferative, pro-apoptotic, and anti-metastatic effects of 2-imino-7-methoxy-4-(4-fluorophenyl)-2h-1,3-thiazine [3,2-a] benzimidazole against pancreatic and melanoma cancer cell lines. Cell viability assays were conducted using Alamar blue assay. Caspase 3/7 activation was evaluated using caspase-Glo® 3/7 substrate reagent. Gene expression was analyzed using conventional polymerase chain reaction (PCR). Cell migration was assessed using wound healing. Alamar blue assay showed that the molecule studied exhibited antiproliferative activity on both the PaCa-2 and A375 cell lines, however, with higher cytotoxicity on PaCa-2 which suggests that it is cell-line dependent. Caspase 3/7 activity was upregulated in PaCa-2 and downregulated in A375, suggesting caspase-dependent and caspase-independent cell death, respectively. p53 and Bax were upregulated on both cell lines which suggests that the compound might have induced apoptosis and autophagy. Wound healing showed a decreased cell migration on both cell lines an important stage of metastasis. The study suggests that the study molecule can be a promising chemotherapeutic agent in the development of new anticancer drugs.

Acta Med Iran 2024;62(September-October):277-289.

Keywords: Cancer; Synthetic compounds; PaCa-2; A375; Anti-proliferation; Pro-apoptosis; Anti-metastatic; Gene expression; p53; Bcl-2; Bax

Introduction

The proliferation of abnormal cells leading to cancer is a serious and life-threatening condition. Sadly, it affects millions of individuals worldwide according to the 2020 global cancer statistics, about 19.3 million new cases were recorded (1,2). Furthermore, in terms of mortality rate about 10 million deaths were estimated in 2020 globally (1). Genetically, cancer is caused by gene alterations, such as the errors that occur when the cells divide, and DNA damage (3). Factors such as age and lifestyle habits, including UV exposure, tobacco smoke, and viruses, can contribute to its mutation (4)

Pancreatic cancer is a concerning disease that affects the pancreas, with common symptoms including jaundice, weight loss, and abdominal pain (5). Unfortunately, the prognosis for pancreatic cancer is poor, with only about 9% of patients living for five years after diagnosis according to the World Health Organization in 2018. In 2020, there were nearly 500,000 new cases and 466,000 deaths reported worldwide (6). The most common type is pancreatic adenocarcinoma,

Corresponding Author: Mpho S. Choene
Department of Biochemistry, Faculty of Science, University of Johannesburg, South Africa
Tel: +98 2142910700, E-mail address: mchoene@uj.ac.za

which accounts for about 90% of cases and begins in the exocrine cells. The development stages of PDAC are known as pancreatic intraepithelial neoplasia (PanIN) and they are classified into three groups PanIN-1A, PanIN-1B, PanIN-2, and PanIN-3 (7). Melanoma skin cancer is defined as the neoplasm of epidermal melanocytes (8). Approximately 325,000 new cases occurred in 2020 with 174,000 for males and 151,000 for females, and if these trends continue, it is estimated that incidence will increase by 50% in 2040 (9). In terms of mortality rate, 57,000 deaths were reported in 2020, and these rates are expected to increase by 68% globally (9). Moreover, overall, 5-year prognosis and survival for melanoma is approximately 94% (10). Superficial spreading melanoma (SSM) is considered the most common type of melanoma and it accounts for about 70% of all cases (11).

The process of apoptosis is very complex, and it involves one of the two pathways: intrinsic (mitochondrial) or extrinsic pathway (12). Activation of apoptosis has been previously documented to be associated with cellular stress stimuli such as chemotherapeutic agents (13). Apoptotic pathways are characterized by the activation of caspase and their activation leads to various morphological changes such as cell blebbing, cell shrinkage, DNA fragmentation, and phagocytosis of apoptotic bodies by neighboring cells (14). During apoptosis mutations may occur in the tumor suppressor gene TP53, and the downregulation of this gene prevents apoptosis from being triggered (15,16). The second mutation may occur in the Bcl-2 proto-oncogene which results in upregulation of Bcl-2 to prevent apoptosis hence promoting cancer progression (17). Successful cancer cell metastasis relies on the ability of cells to escape apoptosis. Cancer cells that have escaped cell death program themselves to gain invasion and migratory properties to metastasize. Approximately 90% of cancer deaths are associated with metastasis worldwide (18,19).

Despite all the efforts in implementing novel chemotherapeutic strategies for all types of cancer, cancer remains a huge concern worldwide. Since the discovery of cancer therapy, these treatments have still failed to cure cancer completely and the prognosis remains poor (20). Chemotherapy, surgery, radiation, and immunotherapy are considered the common types of cancer treatment (21). Challenges with current treatments are mostly related to unspecified symptoms, diagnosis at an advanced stage, re-occurrence, multiple drug resistance, and side effects (22). Synthetic compounds are chemical compounds with a close similarity to natural chemical compounds. However, they differ in property, function, and structure. Thiazine and benzimidazole are heterocyclic organic compounds and their derivatives have been widely used in drug discovery and development because they possess various important pharmaceutical activities including anticancer.

Materials and Methods

Reagents

2 -imino-7-methoxy-4-(4-fluorophenyl)-2h-1,3-thiazine [3,2-a] benzimidazole was obtained from the chemistry department at the University of Johannesburg. Both PaCa-2, A375, and HEK-293 cancer cell lines were donated by Mpho Choene and Lesetja Motadi from the Department of Biochemistry at the University of Johannesburg. high glucose RPMI 1640 medium and trypsin from Thermos Fisher Scientific. Dulbecco phosphate-buffered saline (DPBS) from HyClone, GE Healthcare. Fetal bovine serum (FBS) from HyClone, GE Healthcare. Taxol was obtained from Prof Mutadi (University of Johannesburg). Alamar blue (InvitrogenTM by Thermo Fisher Scientific, Massachusetts, United States). ATP detection substrate reagent from Promega. caspase-Glo® 3/7 substrate reagent from Promega. Hoechst 33342 staining from Thermo Fisher Scientific. Relia-PrepTM RNA-cell MiniPrep kit system from Promega. Goscript TM Reverse Transcriptase system (Promega, Madison, Wisconsin, United States). GoTaq® G2 Green Master Mix from Promega.

Treatment preparation

To prepare a stock solution of 100mg/ml of 2-imino-7-methoxy-4-(4-fluorophenyl)-2h-1,3-thiazine [3,2-a] benzimidazole, the compound was first dissolved in 100% DMSO. The resulting mixture was then used to prepare a 100 µg/ml treatment in high glucose RPMI 1640 medium**.**

Cell culturing

The PaCa-2, A375, and HEK-293 cancer cell lines were donated by Mpho Choene and Lesetja Motadi from the Department of Biochemistry at the University of Johannesburg and cultured in high glucose RPMI 1640 medium, which was enriched with 10% FBS, 1% penicillin-streptomycin, and 0.5µg/ml amphotericin B solution. The cells were kept in a controlled environment at 37˚ C, 5% carbon dioxide, and 95% humidity until they reached 80% confluence. To prepare for the assays, the cells were detached using trypsin-EDTA, counted

with a TC20TM automated cell counter (BIO-RAD, Hercules, California, United States), and then split 1:2 before being returned to the incubator.

Alamar blue cell viability assay

Alamar blue assay was conducted after cell counting and both PaCa-2, A375, and HEK-293 cell lines were first re-suspended with high glucose RPMI 1640 medium in a reservoir using a 10ml serological pipet to obtain the desired concentration of 5 x 10^4 cells/ml. 5000 cells (100 µl) were then seeded into 96 well cell culture plates using a multi-channel pipette. The cells were then incubated for 24 hours using similar conditions as in 2.2. After incubation, the media was discarded, and the cancer cells were washed with DPBS. Different treatments prepared in a media were then added to the cells: (100 µg/ml of 2-imino-7-methoxy-4-(4-fluorophenyl)-2h-1,3-thiazine [3,2-a] benzimidazole, 0.1% of DMSO, and 100 µg/ml taxol). Treated cells were then incubated for 24 hours and added with 10µl of Alamar blue reagent. The cells were then incubated for 24 hours and analyzed using the fluorescence microplate reader (Synergy HT Biotek) machine at 530 mm emission and 590 mm excitation. 2-imino-7-methoxy-4-(4-fluorophenyl)-2h-1,3-thiazine [3,2-a] benzimidazole was then serial diluted from 100 to 3.125 µg/ml and the obtained various concentrations were then tested for cytotoxic activity to obtain an IC50. The cytotoxicity results were analyzed using Excel and the graphs were generated using GraphPad Prism 8.4.3.

Caspase 3/7 activity assay

To conduct a caspase activity assay, 1x105 cell density (2 ml) was first seeded into four 35mm x 12mm cell culture dishes and incubated for 24 hours at 37˚ C in 5% CO2 and 95% humidity for both A375 and PaCa-2 cell lines. The cells were then washed with 500µl of DPBS. Cells were then treated with the following treatments prepared in a media (0.1% of DMSO, 100 µg/ml taxol, IC_{50} for 2-imino-7-methoxy-4-(4-fluorophenyl)-2h-1,3-thiazine [3,2-a] benzimidazole (85.7 µg/ml for PaCa-2 and 98.6 µg/ml for A375 obtained from previous experiment) and incubated for 24 hours. Cells treated with DMSO, and untreated cells, were first washed with 500µl of DPBS. After discarding DPBS, 500 µl of 1x trypsin-EDTA was then added to the dishes to detach cells from the surface. To stop trypsinization, cells were added with 1500 µl of media and transferred into 2 ml Eppendorf tubes. Cells treated with taxol and 2-imino-7-methoxy-4-(4-fluorophenyl)-2h-1,3-thiazine [3,2-a] benzimidazole were transferred into 2ml Eppendorf tubes and the remaining cells in the cell culture dish were added with 100µl of 1 x trypsin-EDTA. To stop trypsinization, cells were added with 400 µl media and transferred into 2 ml Eppendorf tubes. All the tubes were then centrifuged at a speed of 2200 rpm for 2,5 minutes. The supernatant was then discarded, and the cell pellet was added with 500µl of DPBS for washing. The tubes were centrifuged using the same above speed and time. After centrifugation, the cell pellet was re-suspended with 50 µl of the media. Furthermore, 25 µl of the cell's suspension was then loaded into a 96-well black cell culture plate. The cells were then added with 25 µl of caspase-Glo® 3/7 substrate reagent from Promega, (Madison, Wisconsin, United States) and then placed on a rotary shaker for 25 minutes and analyzed using a luminescence microplate reader (Synergy HT Biotek) machine at 405 mm emission.

Microscopic cell morphology assay

To conduct the cell morphology experiment, 1x105 cell density (2 ml) was first seeded into four 35 mm x 12 mm cell culture dishes and pre-incubated for 24 hours at 37˚ C in 5% CO2 and 95% humidity for both A375 and PaCa-2 cell lines. The cells were then washed with 500µl of DPBS and treated with 2ml of treatments (0.1% of DMSO, 100 µg/ml taxol, 2-imino-7-methoxy-4-(4-fluorophenyl)-2h-1,3-thiazine [3,2-a] benzimidazole (98.6 µg/ml of for A375 and 85.7 µg/ml for PaCa-2). For untreated, cells were incubated with media only. After 24 hours of incubation, the cells were visualized and captured using a Leica DM500 microscope (Zeiss, Oberkochen, Baden-Württemberg, Germany) connected to the Leica DM share app on the phone.

Microscopic fluorescence Hoechst 33342 staining assay

The cell density of 1x10^5 (2 ml) was first seeded into four 35mm x 12mm cell culture dishes and incubated for 24 hours for both A375 and PaCa-2 cell lines. The cells were then washed with 500 µl of DPBS and treated with 2ml of treatments (0.1% of DMSO, 100µg/ml taxol, 2-imino-7-methoxy-4-(4-fluorophenyl)-2h-1,3-thiazine [3,2-a] benzimidazole (98.6 µg/ml of for A375 and 85.7µg/ml for PaCa-2). Untreated cells were incubated with media only. After 24 hours of incubation, cells treated with taxol and 2-imino-7-methoxy-4-(4-fluorophenyl)-2h-1,3-thiazine [3,2-a] benzimidazole were transferred into 2 ml Eppendorf tubes. cells treated with DMSO, and untreated cells were first washed with 500 µl of DPBS. After discarding DPBS, 500 µl of 1x trypsin-EDTA was added to the dishes to detach cells from the surface. To stop trypsinization, cells were added

with 1500 µl of media and transferred into 2 ml Eppendorf tubes. All the tubes were then centrifuged at a speed of 2200 rpm for 2,5 minutes. The supernatant was then discarded, and the cell pellet was added with 500µl of DPBS for washing. The tubes were again centrifuged at 2200 rpm for 2,5 minutes. Hoechst 33342 stain from Thermos Fisher Scientific was diluted in DPBS by a 1:2000 ratio. The final concentration of Hoechst stain in DPBS was 0.5 µg/ml. After centrifugation, the cell pellet was re-suspended with 50µl of Hoechst stain solution and incubated for 5-10 minutes. After incubation time, 15 µl of the cells were then loaded into 76 x 26 mm slides and closed on top with a 22 x 22 cover slip and read using a fluorescence microscope using 350 nm excitation and 461nm emission, and the images were captured using 10x, 20x and 40x magnification.

RNA extraction

Both untreated and treated RNA from PaCa-2 and A375 cell lines were extracted and purified using the Relia-PrepTM RNA-cell MiniPrep kit system from Promega (Madison, Wisconsin, United States) as per manufacture protocol for about 24 hours. To conduct this experiment, 1x105 cell density (2 ml) was first seeded into two 35mm x 12mm cell culture dishes and pre-incubated for 24 hours at 37˚ C in 5% of CO2 and 95% humidity for both A 375 and PaCa-2 cell lines. The cells were then washed with 500 µl of DPBS and treated with 2ml of treatment (2-imino-7-methoxy-4-(4-fluorophenyl)-2h-1,3-thiazine [3,2-a] benzimidazole (98.6µg/ml of for A375 and 85.7µg/ml for PaCa-2). For untreated, cells were incubated with media only. After 24 hours of incubation, the media was discarded, and the cells were added with 1ml of lysis buffer and 10µl of 1-Thioglycerol and transferred into a 2 ml Eppendorf tube. The cells were stored at -80˚ C overnight. The cell lysate was then thawed on ice and later vortex for five minutes. 1 ml of 70% ethanol was then added to the lysate and vortexed for a minute. 700 µl of the sample was then transferred into a spin centrifuge with a collection tube and harvested by centrifugation at 12000 x g for one minute and the liquid on the collection tube was discarded. This was repeated until the solution on the initial tube was finished. 700 µl of the wash buffer I was then added into the spin collection and centrifuged for one minute at 12000 x g. The spin collection was then transferred into a new collection tube and added with 500 µl of wash buffer II with ethanol and centrifuged again for one minute at 12000 x g. This step was repeated twice, and the spin centrifuge was centrifuged on its own without a collection tube for three minutes at 12000 x g to dry the membrane-bound with the RNA. To elute the RNA, 80µl of the RNAse-free water was added to the center of the spin centrifuge this time with a new collection tube and incubated at room temperature for a minute. After incubation, it was centrifuged at 12000 x g for two minutes. The spin centrifuge was then removed, and the RNA was transferred into the recovery tube. The purity was then determined using Nano-Drop at A260/A280 ratio and stored at -80˚ C.

RT-Polymerase chain reaction (PCR)

Reverse transcription was performed using the Goscript™ Reverse Transcriptase system from Promega. To synthesize cDNA, different components were mixed to make a total volume of 20 µl reaction. Firstly, the RNA primer mix was prepared and spun down using a quick-spin mini centrifuge to allow the solution to settle at the bottom of the tube. The mixture was then heated at 70° C for 5 minutes using the AccuBlock™ heating block from Labnet, followed by quick chilling on ice for about 2-5 minutes until the reverse transcription master mix was prepared. Next, the reverse transcription master mix was added to the tube containing the RNA primer mixture solution, and the combined mixture was incubated under thermal cycling conditions using a PCR master cycler. The resulting cDNA was then used for PCR amplification. For amplification, GoTaq® G2 Green Master Mix from Promega was used to make a 10 µl total volume of cDNA and primer mix. The samples were incubated under thermal cycling conditions for amplification using the PCR Master cycle. The cycle conditions were repeated for 40 cycles, and the PCR products (amplicons) were electrophoresed using agarose gel electrophoresis.

Gel electrophoresis

Gel electrophoresis was performed in this study to assess the effectiveness of the primers. To run the samples, 1% agarose gel was used. To prepare the gel, 1g of agarose was dissolved in 100 ml of 1 x TAE buffer (40 mM Tris pH 8; 45 mM acetic acid; 1 mM EDTA) and heated in a microwave for 60 seconds. After cooling down, 10µl of ethidium bromide was added to solidify the solution. Subsequently, 3 µl of DNA ladder and 10 µl of the PCR product solution were loaded onto the agarose gel immersed in 1 x TAE buffer. The samples were then electrophoresed for 40 minutes at 100 volts, and the Gel Doc (Bio-Rad) machine was used to detect the bands. Bio-Rad Image Lab software 6.1 was employed to quantify the bands and obtain their intensity values for each gene.

Wound healing assay

To perform a wound healing assay, first, 100 µl of PaCa-2 and A375 cell lines were diluted in RPMI media to achieve the correct seeding density. Then, 1x105 cell density (2 ml) cells were seeded into four 35 mm x 12mm cell culture dishes and incubated overnight at 37° C in 5% CO2 and 95% humidity, allowing them to adhere. When the cells reached 80% confluency, the media was discarded without disturbing the cells. The cells were then washed with 1x DPBS, and a scratch was made from the top to the bottom of each petri dish using a p20 micropipette tip. Next, the cells were treated with 2 ml of treatments (0.1% DMSO, 100 µg/ml taxol, 2-imino-7-methoxy-4-(4-fluorophenyl)-2h-1,3-thiazine [3,2-a] benzimidazole (98.6 µg/ml for A375 and 85.7 µg/ml for PaCa-2), and incubated for 24 hours to inhibit cell migration. For untreated cells, only media was added, and they were incubated similarly. The Leica DM500 microscope was used to capture images at 10x magnification, and the results were analyzed by measuring the distance between two margins of the gap on different wound areas before and after 24 hours, 48 hours, and 72 hours of incubation with treatments. Additionally, the cellular migration rate of each treatment was compared to that of untreated cells.

Statistical analysis

The results were represented as the mean of two independent experiments±standard error concerning untreated and the p-value was calculated in comparison to the control. The $P<0.05$ is typically considered statistically significant which indicates strong evidence against the null hypothesis.

Table 1. Oligonucleotide primers used for real-time RT-PCR analysis

Gene	Forward primer	Reverse primer	Length bp)
P53	5'GTATTTCACCCTCAAGATCC- 3′	5′- TGGGCATCCTTTAACTCTA -3′	124
Bax	5′- CTACAGGGTTTCATCCAG -3′	5′- CCAGTTCATCTCCAATTCG -3′	133
Bcl2	5′- GTGGATGACTGAGTACCT -3′	5′- CCAGGAGAAATCAAACAGAG -3′	118
B-actin	5′- GAGAAACCTGCCAAGTATG -3′	5′- GGAGTTGCTGTTGAAGTC -3′	155

Results

Cytotoxicity screening of various synthetic compounds on PaCa-2 and A375

To study anticancer activity, synthesized 1,3-thiazine [3,2-a] benzimidazole and its derivatives were first screened at 100µg/ml against PaCa-2 and A375 cell lines for 24 hours using Alamar blue™ cell viability assay. As shown in Figure 1, 2nd derivative which is identified as 2-imino-7-methoxy-4-(4-fluorophenyl)-2h-1,3-thiazine [3,2-a] benzimidazole exhibited the greatest cytotoxicity as compared to both cell line hence it was selected for this study.

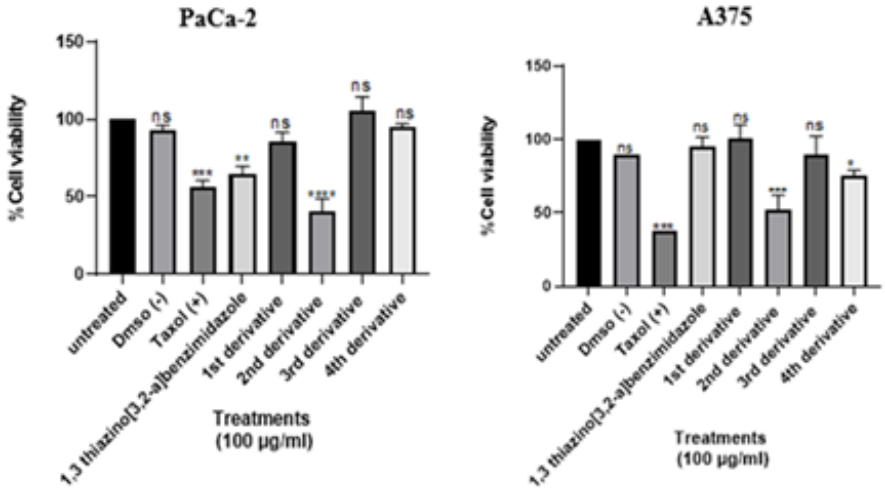

Figure 1. Cytotoxic screening activity of 1,3-thiazine [3,2-a] benzimidazole derivatives at 100µg/ml on PaCa-2 and A375 cells

Five different compounds were tested for anti-proliferative activity at a final concentration of 100 µg/ml. Untreated represents cells with media only; for negative control, cells were treated with 0.1% total concentration of DMSO. For positive control, cells were treated with 100 µg/ml final concentration of taxol supplemented with RPMI media. The results were obtained using a fluorescence microplate reader (Synergy HT Biotek) and represented as the mean of two independent experiments±standard error regarding untreated and submitted to one-way ANOVA with Dunnett's multiple comparisons test ****P<0,0001 (PaCa-2) and ***P=0,0001 (A375).

Cytotoxicity of 2-imino-7-methoxy-4-(4-fluorophenyl)-2h-1,3-thiazino [3,2-a] benzimidazole

The structure of 2-imino-7-methoxy-4-(4-fluorophenyl)-2h-1,3-thiazine [3,2-a] benzimidazole has been shown below in Figure 2A**.** To examine the anti-proliferative activity of 2-imino-7-methoxy-4-(4-fluorophenyl)-2h-1,3-thiazine [3,2-a] benzimidazole, HEK-293 cell line, PaCa-2 and A375 cells were treated with (100, 50, 25, 12.5, 6.25, and 3.125 µg/ml) for 24 hours and the cell viability was measured by Alamar Blue assay. As shown in Figure 2B, 2-imino-7-methoxy-4-(4-fluorophenyl)-2h-1,3-thiazine [3,2-a] benzimidazole exhibited the greatest inhibitory activity at 100µg/ml on PaCa-2 and A375 cancer cells whereas on non-cancerous cells (HEK-293) show a partial activity.

(A) is the structure of 2-imino-7-methoxy-4-(4-fluorophenyl)-2h-1,3-thiazino [3,2-a] benzimidazole. (B) is Various concentrations of 2-imino-7-methoxy-4-(4-fluorophenyl)-2h-1,3-thiazine [3,2-a] benzimidazole from a final concentration of 100µg/ml to 3.125µg/ml were tested for antiproliferative activity against HEK-293 cells, PaCa-2 and A375. Untreated represents cells with media only; for negative control, cells were treated with 0.1% final concentration of DMSO. For positive control, cells were treated with 100µg/ml taxol. The numbers from 100µg/ml to 3.125µg/ml on the x-axis are various concentrations of 2-imino-7-methoxy-4-(4-fluorophenyl)-2h-1,3-thiazine [3,2-a] benzimidazole). The results were obtained using a fluorescence microplate reader (Synergy HT Biotek) and represented as the mean of two independent experiments ± standard error concerning untreated and submitted to one-way ANOVA with Dunnett's multiple comparisons tests ***P=0,0012* (HEK-293), ****P<0,0001* (PaCa-2), *** *P=0,0008* (A375).

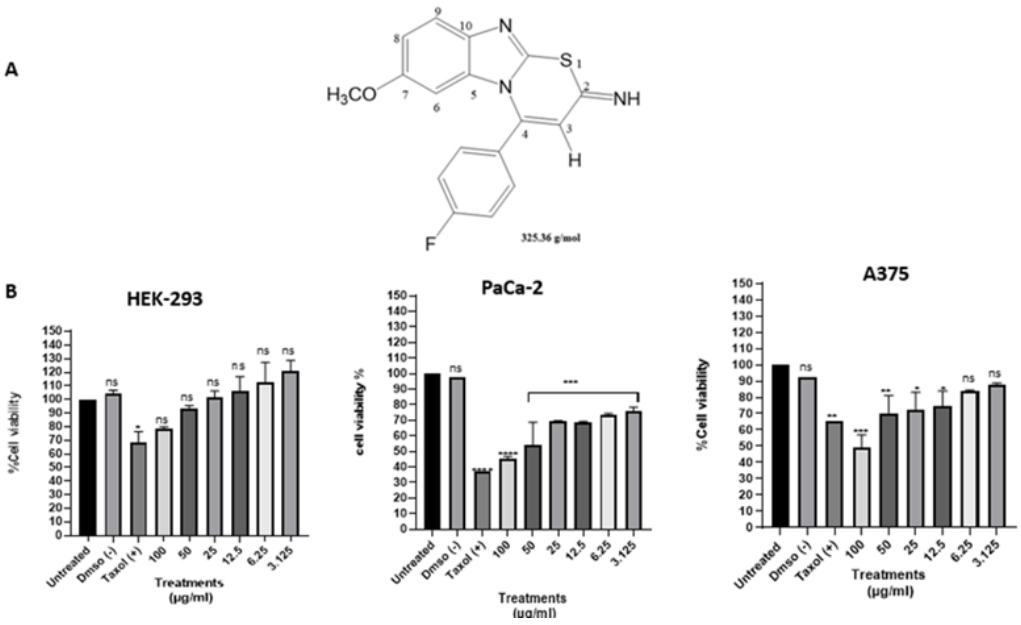

Figure 2. Cytotoxic activity of 2-imino-7-methoxy-4-(4-fluorophenyl)-2h-1,3-thiazino [3,2-a] benzimidazole on HEK-293 cell line, PaCa-2 and A375

Caspase 3/7 induction with IC50 for 2-imino-7-methoxy-4-(4-fluorophenyl)-2h-1,3-thiazino [3,2-a] benzimidazole

To evaluate the pro-apoptotic activity of 2-imino-7-methoxy-4-(4-fluorophenyl)-2h-1,3-thiazino [3,2-a] benzimidazole, PaCa-2 and A375 were treated for 24 hours with 85.7 and 98.6µg/ml IC50 of 2-imino-7-methoxy-4-(4-fluorophenyl)-2h-1,3-thiazino [3,2-a] benzimidazole, respectively. Caspase 3/7 activity was measured using luminescent caspase-Glo® 3/7 substrate. As shown in Figure 3, caspases 3 and 7 were upregulated in PaCa-2 only whereas in A375 were significantly dropped.

An IC_{50} of 85.7 µg/ml and 98.6 µg/ml of 2-imino-7-methoxy-4-(4-fluorophenyl)-2h-1,3-thiazine [3,2-a] benzimidazole was tested on Paca-2 and A375 cells, respectively, for pro-apoptotic activity based on luminescence caspase 3/7 activity. For negative control, cells were treated with 0.1% of DMSO, for positive control, cells were treated with 100µg/ml taxol. The final concentration of 85.7 µg/ml on the x-axis is an IC_{50} value of 2-imino-7-methoxy-4-(4-fluorophenyl)-2h-1,3-thiazine [3,2-a] benzimidazole. The luminescence results were obtained using synergy HT Biotek and were represented as the mean of two independent experiments ± standard error concerning untreated and submitted to one-way ANOVA with Dunnett's multiple comparisons test ***P=0.0064* (PaCa-2), ****P=0.0001* (A375).

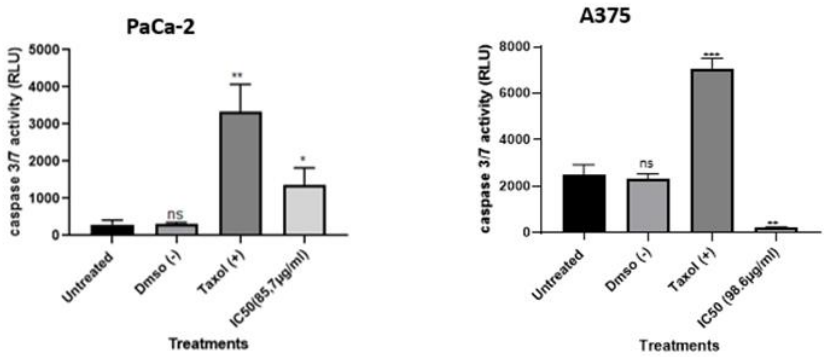

Figure 3. Caspase 3/7 activity induced with IC50 of 2-imino-7-methoxy-4-(4-fluorophenyl)-2h-1,3-thiazino [3,2-a] benzimidazole on PaCa-2 and A375 cells

Microscopic analysis on PaCa-2 and A375 after treatment with 2-imino-7-methoxy-4-(4-fluorophenyl)-2h-1,3-thiazino [3,2-a] benzimidazole

To investigate cell morphological effects of 2-imino-7-methoxy-4-(4-fluorophenyl)-2h-1,3-thiazino [3,2-a] benzimidazole, PaCa-2 and A375 were treated with IC50 for 2-imino-7-methoxy-4-(4-fluorophenyl)-2h-1,3-thiazino [3,2-a] benzimidazole for 24 hours. The changes in cell shape and nucleus were investigated using Leica DM500 microscope and fluorescence Hoechst staining, respectively. As shown in Figure 4A both cell lines changed their shape from spindle to round after the treatment. In Figure 4B, PaCa-2 cells showed nuclear fragmentation after treatment with 2-imino-7-methoxy-4-(4-fluorophenyl)-2h-1,3-thiazino [3,2-a] benzimidazole whereas most of the A375 cell's nucleus shrinks without showing fragmentation

Images were obtained using the Leica DM500 microscope and fluorescence microscopy showing the changes in the cells' shape and nucleus respectively after 24 hours of incubation with/without exposure to IC50 for 2-imino-7-methoxy-4-(4-fluorophenyl)-2h-1,3-thiazine [3,2-a] benzimidazole. Figure 5A is a microscopic analysis, Figure 5B is fluorescence Hoechst staining, 0.1% DMSO represents the negative control whereas the 100 µg/ml Taxol represents the positive control.

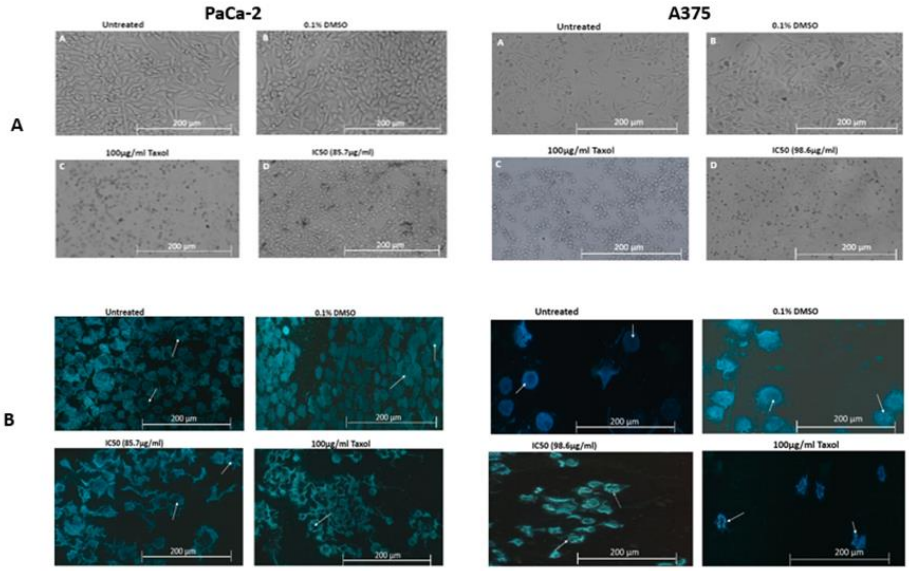

Figure 4. Microscopic analysis on PaCa-2 and A375 cells

Effects of 2-imino-7-methoxy-4-(4-fluorophenyl)-2h-1,3-thiazino [3,2-a] benzimidazole on apoptotic Gene expression on PaCa-2 and A375 cell lines

The apoptotic gene expression (p53, Bax, and Bcl-2) was evaluated using conventional PCR and analyzed using gel electrophoresis to check the efficiency of the primers. As shown in Figure 5A and Figure 5B, the housekeeping gene *β-actin* as expected exhibited the same trend as control. Again, as shown in Figure 6A and Figure 6B, an IC50 for 2-imino-7-methoxy-4-(4-fluorophenyl)-2h-1,3-thiazino [3,2-a] benzimidazole significantly upregulated the expressional level of p53 and Bax on both PaCa-2 and A375. The Bcl-2 was downregulated on both cell lines as shown in Figures 5A and B.

For both agarose gels, M represents the marker, 1st band represents *β-actin* (housekeeping gene), 2nd represents *p53*, 3rd represents *Bcl2*, and 4th represents *Bax*. The results were represented as the mean of two independent experiments±standard error with reference to untreated and submitted to one-way ANOVA with Dunnett's multiple comparisons test ****$P<0,0001$.

For both agarose gels, M represents the marker, 1st band represents β-actin (housekeeping gene, 2nd represents p53, 3rd represents Bcl2, and 4th represents Bax represented as the mean of two independent experiments±standard error with reference to untreated and submitted to one way ANOVA with Dunnett's multiple comparisons test ****P<0,0001.

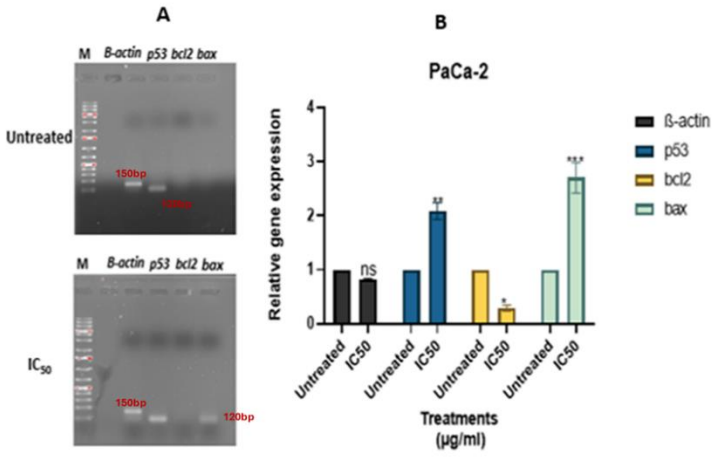

Figure 5A. RT-PCR products resolved on agarose gel showing the expressional level of genes on PaCa-2 cells after treatment with IC_{50} (85.7 µg/ml) of 2-imino-7-methoxy-4-(4-fluorophenyl)-2h-1,3-thiazino [3,2-a] benzimidazole

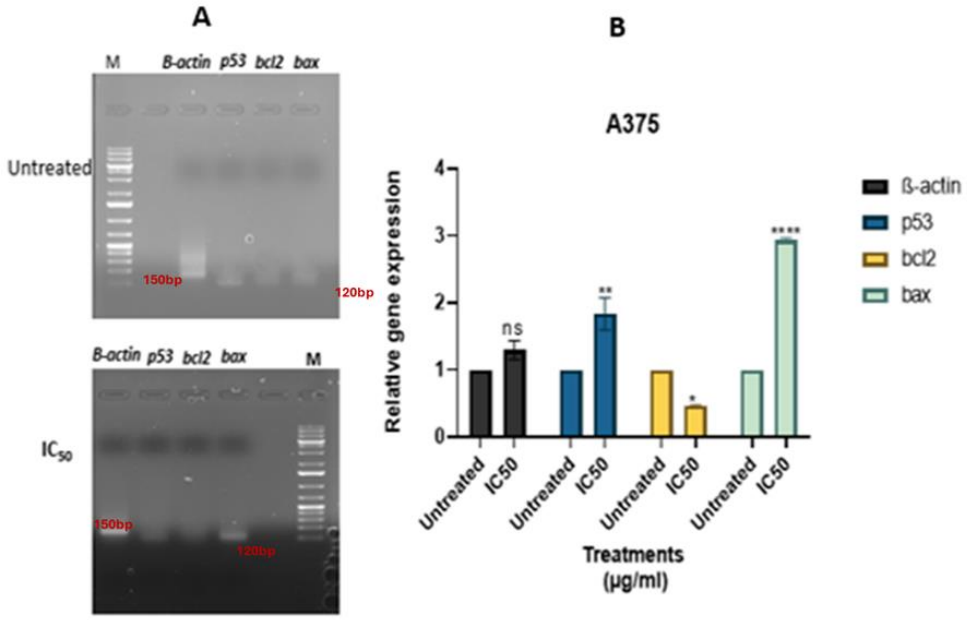

Figure 5B. RT-PCR products resolved on agarose gel showing the expressional level of genes on A375 cells after treatment with IC50 (98.6 µg/ml) of 2-imino-7-methoxy-4-(4-fluorophenyl)-2h-1,3-thiazine [3,2-a] benzimidazole

Cellular migratory effects of 2-imino-7-methoxy-4-(4-fluorophenyl)-2h-1,3-thiazino [3,2-a] benzimidazole on PaCa-2, and A375 cell lines

To examine the anti-metastatic activity of 2-imino-7-methoxy-4-(4-fluorophenyl)-2h-1,3-thiazine [3,2-a] benzimidazole, HEK-293 cell line, PaCa-2, and A375 cells were treated for 0 hour, 24 hours, 48 hours and 72 hours 24 hours with 85.7 and 98.6 µg/ml IC50 for of 2-imino-7-methoxy-4-(4-fluorophenyl)-2h-1,3-thiazine [3,2-a] benzimidazole and cell migration was measured using wound healing assay. As shown in Figure 6, 2-imino-7-methoxy-4-(4-fluorophenyl)-2h-1,3-thiazine [3,2-a] benzimidazole exhibited greater migratory activity as compared to control on both PaCa-2 and A375 cell lines.

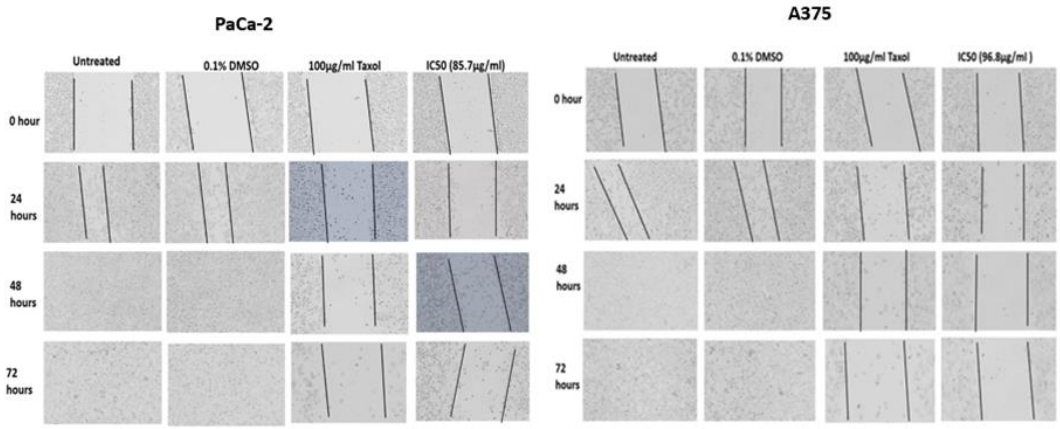

Figure 6. Cellular migration on PaCa-2 and A375 cells after treatment with 2-imino-7-methoxy-4-(4-fluorophenyl)-2h-1,3-thiazino [3,2-a] benzimidazole

The results were presented as images captured by a Leica DM500 microscope to show the migration rate obtained by measuring the distance between two margins of the gap at times 0hour, 24hour, 48hours and 72hours with/without the exposure to IC50 for 2-imino-7-methoxy-4-(4-fluorophenyl)-2h-1,3-thiazine [3,2-a] benzimidazole. 0.1% of DMSO represents the negative control whereas the 100µg/ml taxol represents the positive control.

Discussion

This study tested the effects of 2-imino-7-methoxy-4-(4-fluorophenyl)-2h-1,3-thiazino [3,2-a] benzimidazole on PaCa-2 and A375 cell lines. The aim was to measure its ability to reduce cell proliferation, promote apoptosis, and inhibit metastasis in vitro. Results showed that the compound was effective in achieving these objectives. The molecular weight of the compound was found to be 325.36 g/mol, making it a small molecule that can be used as a target chemotherapy drug for cancer treatments. 2-imino-7-methoxy-4-(4-fluorophenyl)-2h-1,3-thiazine [3,2-a] benzimidazole was prepared using 100% DMSO, but the treatments were made using 0.1% DMSO to avoid cell death caused by DMSO. However, 0.1% to 0.5% DMSO is considered safe for cells, while concentrations higher than 1% can be cytotoxic (23). Taxol was used as a positive control and a concentration of 100 µg/ml was previously shown to have high inhibitory activity on both PaCa-2 and A375 cell lines (24).

A study was conducted to test the antiproliferative effects of 1,3-thiazine [3,2-a] benzimidazole and its derivatives on cancer cell lines using the Alamar blue cytotoxicity assay. Cytotoxic activity test is regarded as a crucial step in cell culture because it measures the degree to which the test molecules will be able to cause cell death, regardless of the cell type it is crucial to know the number of viable or non-viable cells at the end of the experiment (25). Among the tested compounds, 2-imino-7-methoxy-4-(4-fluorophenyl)-2h-1,3-thiazine [3,2-a] benzimidazole showed the highest inhibitory activity. The parent compound 1,3-thiazine [3,2-a] benzimidazole showed the lowest inhibitory activity on PaCa-2, suggesting that additional functional groups might have upregulated its activity. Synthetic derivatives of 1,3-thiazine [3,2-a] benzimidazole have been reported to have anti-tuberculosis activity (26) and antioxidant activity (27). However, it has never been characterized or tested against cancer cells. Various concentrations of 2-imino-7-methoxy-4-(4-fluorophenyl)-2h-1,3-thiazine [3,2-a] benzimidazole were tested against normal and cancer cells to obtain an IC_{50}. IC_{50} value for a pure drug is less than 20µg/ml and is considered potent (28,29). However, it was also documented that an IC_{50} value between 20 and 100 µg/ml exhibits moderate cytotoxic activity, and it can be used for a study (29). Furthermore, an IC_{50} greater than 100 µg/ml is considered non-active (28). IC_{50} value for this compound was found to be 85.7µg/ml and 98.6 µg/ml for PaCa-2 and A375, respectively. HEK-293 was used as a normal cell in this study. HEK-293 has been widely used for cancer research as a normal cell line, protecting non-cancerous cells has been reported to increase therapeutic outcomes whereas killing them limits cancer chemotherapy (30,31). The IC_{50} value of 168 µg/ml against HEK-293 suggests that this compound might be non-toxic to non-cancerous cells.

Effector caspase 3 and 7 are well-known executioner proteins and their activation is considered key mediators to the late stage of apoptosis (32). Furthermore, effector caspases 3/7 are now being used as a primary target to test the effectiveness of potential anticancer drugs (33). In this study, the IC_{50} value of 2-imino-7-methoxy-4-(4-fluorophenyl)-2h-1,3-thiazine [3,2-a] benzimidazole upregulated caspases 3 and 7 on PaCa-2 cells only, an evident that PaCa-2 cell death is caspase-dependent and apoptotic. In A375 cell lines, caspase 3/7 activity significantly dropped suggesting caspase-independent cell death. Several studies have shown that cell death can occur through mechanisms that do not involve caspase activation, including autophagy (34).

Studying morphological changes provides very crucial information about cells including cell function, differentiation process, and signal response. Activation of executioner caspases has been documented to result in morphological changes such as cell blebbing, cell shrinkage, DNA fragmentation, and phagocytosis of apoptotic bodies by neighbouring cells (14). Caspase-independent cell death has been reported to share the same characteristics as caspase-dependent cell death except that it does not involve nuclear fragmentation (35). In this study, the IC_{50} value of 2-imino-7-methoxy-4-(4-fluorophenyl)-2h-1,3-thiazine [3,2-a] benzimidazole has shown morphological effects on focus cancer cell lines, both PaCa-2 and A375 changed their shape from spindle to round. Cancer cells are known to have well-formed nuclei and condensed DNA (36). In this study, most of the PaCa-2 cells exhibited nuclear fragmentation after treatment, which validated caspase activity results that suggested that cells are undergoing caspase-dependent cell death. In contrast, most of the A375 cells shrink

without fragmentation. Nuclear shrinkage without fragmentation has been documented as one of the characteristics of caspase-independent cell death (35).

Gene expression analysis was carried out to study three apoptotic-related genes, p53, Bcl-2, and Bax using conventional PCR. Many studies have reported these genes to play a significant role in the intrinsic apoptotic pathway (37,38). In this study a housekeeping gene *β-actin* was used as a control to ensure accurate expression analysis of the gene of interest. The *p53* gene is a tumor suppressor gene and its expression has been found crucial in regulating cell death including apoptosis (39). *Bcl-2* is a pro-survival gene, and its expression has been documented to inhibit apoptosis in many cancer cells by directly inhibiting the expression of pro-apoptotic genes such as *Bax* and *Bak* (40). The downregulation of Bcl-2 has been reported to occur through various mechanisms, including expression of p53, upregulation of Bax, and caspase-independent autophagy [41,42,43]. *Bax* is a member of *Bcl-2* known as a pro-apoptotic gene, a key regulator of the apoptotic intrinsic pathway and its expression has been reported to promote apoptosis by inducing the release of cytochrome C crucial for caspase activation and ultimately cell death (44,45,34). The expression of *Bax* alone has also been documented to stimulate autophagy in cancer cells (44,46). Cancer cells expressing *Bax* can undergo caspase-independent cell death due to various factors such as TRAIL and caspase inhibitors (44,46). However, the mechanism of regulating this type of cell death remains unclear. For this study, the upregulation of Bax on A375 suggests autophagy. The results obtained for PaCa-2 showed an upregulation of p53 and Bax and a downregulation of Bcl-2 after treatment, which suggests that the observed cell death is apoptotic and p53-dependent. In this study, *Bcl-2* was downregulated on both focus cell lines after treatment which suggests an increase in apoptosis and autophagy.

The study investigated the anti-metastatic effects of 2-imino-7-methoxy-4-(4-fluorophenyl)-2h-1,3-thiazine [3,2-a] benzimidazole on PaCa-2 and A375 cells using a wound healing assay. The results suggest that this compound suppresses migration on both cell lines and exhibits greater migratory activity

The experimental findings demonstrated that the compound reduced cell proliferation in both cell lines, with higher cytotoxicity towards PaCa-2, indicating cell-line dependency. It induced both caspase-dependent and caspase-independent cell death for PaCa-2 and A375, respectively, with p53-dependent cell death. The expression of Bax was promoted on both cell lines, suggesting the induction of apoptosis and autophagy on PaCa-2 and A375, respectively. The wound healing assay concluded that the compound inhibits metastasis on both cell lines, suggesting its potential as a promising chemotherapeutic agent. However, further research is needed to understand the mechanism of action and the relationship between Bax expression and caspase-independent cell death in cancer cells. The compound's anticancer properties can be further investigated through in vivo studies and other cancer cell lines.

References

1. Arnold M, Singh D, Laversanne M, Vignat J, Vaccarella S, Meheus F, Cust AE, et al. Global burden of cutaneous melanoma in 2020 and projections to 2040. JAMA Dermatol 2022;158:495-503.
2. Ferlay J, Colombet M, Soerjomataram I, Parkin DM, Piñeros M, Znaor A, et al. Cancer statistics for the year 2020: An overview. Int J Cancer 2021;149:778-89.
3. Loeb KR, Loeb LA. Significance of multiple mutations in cancer. Carcinogenesis 2000;21:379-85.
4. Takeshima H, Ushijima T. Accumulation of genetic and epigenetic alterations in normal cells and cancer risk. NPJ Precis oncol 2019;3:7.
5. Porta M, Fabregat X, Malats N, Guarner L, Carrato A, De Miguel A, et al. Exocrine pancreatic cancer: symptoms at presentation and their relation to tumour site and stage. Clin Transl Oncol 2005;7:189-97.
6. Ilic I, Ilic M. International patterns in incidence and mortality trends of pancreatic cancer in the last three decades: a joinpoint regression analysis. World J Gastroenterol 2022;28:4698-715.
7. Martin A, Cros J, Vullierme MP, Dokmak S, Sauvanet A, Levy P, et al. Dilatation of the main pancreatic duct of unknown origin: causes and risk factors of pre-malignancy or malignancy. Surg Endosc 2023;37:3684-90.
8. Rashid S, Shaughnessy M, Tsao H. Melanoma classification and management in the era of molecular medicine. Dermatol Clin 2023;41:49-63.
9. Arnold M, Singh D, Laversanne M, Vignat J, Vaccarella S, Meheus F, Cust AE, et al. Global burden of cutaneous melanoma in 2020 and projections to 2040. JAMA Dermatol 2022;158:495-503.
10. Siegel RL, Miller KD, Wagle NS, Jemal A. Cancer statistics, 2023. Ca Cancer J Clin 2023;73:17-48.
11. Mitchell TC, Karakousis G, Schuchter L. Melanoma. InAbeloff's Clinical Oncology 2020 Jan 1 (pp. 1034-1051). Elsevier.
12. Ghobrial IM, Witzig TE, Adjei AA. Targeting apoptosis pathways in cancer therapy. CA Cancer J Clin 2005;55:178-94.

13. Fulda S, Gorman AM, Hori O, Samali A. Cellular stress responses: cell survival and cell death. Int J Cell Biol 2010:2010:214074.
14. Elmore S. Apoptosis: a review of programmed cell death. Toxicol Pathol 2007;35:495-516.
15. Borrero LJ, El-Deiry WS. Tumor suppressor p53: Biology, signaling pathways, and therapeutic targeting. Biochim Biophys Acta Rev Cancer 2021;1876:188556.
16. Kontomanolis EN, Koutras A, Syllaios A, Schizas D, Mastoraki A, Garmpis N, et al. Role of oncogenes and tumor-suppressor genes in carcinogenesis: a review. Anticancer Res 2020;40:6009-15.
17. Sarkar A, Paul A, Banerjee T, Maji A, Saha S, Bishayee A, et al. Therapeutic advancements in targeting BCL-2 family proteins by epigenetic regulators, natural, and synthetic agents in cancer. Eur J Pharmacol 2023;944:175588.
18. Mitchell TC, Karakousis G, Schuchter L. Melanoma. InAbeloff's Clinical Oncology 2020 Jan 1 (pp. 1034-1051). Elsevier.
19. Monteiro J, Fodde R. Cancer stemness and metastasis: therapeutic consequences and perspectives. European J Cancer 2010;46:1198-203.
20. Debela DT, Muzazu SG, Heraro KD, Ndalama MT, Mesele BW, Haile DC, et al. New approaches and procedures for cancer treatment: Current perspectives. SAGE Open Med 2021;9:20503121211034366.
21. Siegel R, DeSantis C, Virgo K, Stein K, Mariotto A, Smith T, et al. Cancer treatment and survivorship statistics, 2012. CA Cancer J Clin 2012;62:220-41.
22. Zhang L, Sanagapalli S, Stoita A. Challenges in diagnosis of pancreatic cancer. World J Gastroenterol 2018;24:2047-60.
23. Hajighasemi F, Tajic S. Assessment of cytotoxicity of dimethyl sulfoxide in human hematopoietic tumor cell lines. Iran J Blood Cancer 2017;9:48-53.
24. Zandi M. Cytotoxicity of taxol in combination with vincristine and vinblastine against A375 cell line. Gene Cell Tissue 2021;8:e114359.
25. Adan A, Kiraz Y, Baran Y. Cell proliferation and cytotoxicity assays. Curr Pharm Biotechnol 2016;17:1213-21.
26. Gong JX, He Y, Cui ZL, Guo YW. Synthesis, spectral characterization, and antituberculosis activity of thiazino [3, 2-A] benzimidazole derivatives. Phosphorus Sulfur Silicon Relat Elements 2016;191:1036-41.
27. Rodríguez OA, Vergara NE, Sánchez JP, Martínez MT, Sandoval ZG, Cruz A, et al. Synthesis, crystal structure, antioxidant activity and dft study of 2-aryl-2, 3-dihydro-4H-[1, 3] thiazino [3, 2-a] benzimidazol-4-One. Molecules 2014;19:8414-33.
28. Bero J, Beaufay C, Hannaert V, Hérent MF, Michels PA, Quetin-Leclercq J. Antitrypanosomal compounds from the essential oil and extracts of Keetia leucantha leaves with inhibitor activity on Trypanosoma brucei glyceraldehyde-3-phosphate dehydrogenase. Phytomedicine 2013;20:270-4.
29. Larayetan R, Ololade ZS, Ogunmola OO, Ladokun A. Phytochemical constituents, antioxidant, cytotoxicity, antimicrobial, antitrypanosomal, and antimalarial potentials of the crude extracts of Callistemon citrinus. Evid Based Complement Alternat Med 2019:2019:5410923.
30. Apontes P, Leontieva OV, Demidenko ZN, Li F, Blagosklonny MV. Exploring long-term protection of normal human fibroblasts and epithelial cells from chemotherapy in cell culture. Oncotarget 2011;2:222-33.
31. Johari SA, Sarkheil M, Veisi S. Cytotoxicity, oxidative stress, and apoptosis in human embryonic kidney (HEK293) and colon cancer (SW480) cell lines exposed to nanoscale zeolitic imidazolate framework 8 (ZIF-8). Environ Sci Pollut Res Int 2021;28:56772-81.
32. McKenzie BA, Fernandes JP, Doan MA, Schmitt LM, Branton WG, Power C. Activation of the executioner caspases-3 and-7 promotes microglial pyroptosis in models of multiple sclerosis. J Neuroinflammation 2020;17:253.
33. Yadav P, Yadav R, Jain S, Vaidya A. Caspase- 3: a primary target for natural and synthetic compounds for cancer therapy. Chem Biol Drug Des 2021;98:144-65.
34. Perfettini JL, Reed JC, Israël N, Martinou JC, Dautry-Varsat A, Ojcius DM. Role of Bcl-2 family members in caspase-independent apoptosis during Chlamydia infection. Infect Immun 2002;70:55-61.
35. Tait SW, Green DR. Caspase-independent cell death: leaving the set without the final cut. Oncogene 2008;27:6452-61.
36. Zhang YP, Li YQ, Lv YT, Wang JM. Effect of curcumin on the proliferation, apoptosis, migration, and invasion of human melanoma A375 cells. Genet Mol Res 2015;14:1056-67.
37. Güllülü Ö, Hehlgans S, Rödel C, Fokas E, Rödel F. Tumor suppressor protein p53 and inhibitor of apoptosis proteins in colorectal cancer—A promising signaling network for therapeutic interventions. Cancers (Basel) 2021;13:624.
38. Gupta S, Kass GE, Szegezdi E, Joseph B. The mitochondrial death pathway: a promising therapeutic target in diseases. J Cell Mol Med 2009;13:1004-33.
39. CC H. Clinical implications of the p53 tumor-suppressor gene. N Engl J Med 1993;329:1318-27.
40. Xu Y, Ye H. Progress in understanding the mechanisms of resistance to BCL-2 inhibitors. Exp Hematol Oncol 2022;11:31.
41. Haldar S, Negrini M, Monne M, Sabbioni S, Croce CM.

Down-regulation of bcl-2 by p53 in breast cancer cells. Cancer Res 1994;54:2095-7.

42. Naseri MH, Mahdavi M, Davoodi J, Tackallou SH, Goudarzvand M, Neishabouri SH. Up regulation of Bax and down regulation of Bcl2 during 3-NC mediated apoptosis in human cancer cells. Cancer Cell Int 2015;15:55.
43. Saeki K, Yuo A, Okuma E, Yazaki Y, Susin SA, Kroemer G, et al. Bcl-2 down-regulation causes autophagy in a caspase-independent manner in human leukemic HL60 cells. Cell Death Differ 2000;7:1263-9.
44. Kögel D, Prehn JH. Caspase-independent cell death mechanisms. InMadame Curie Bioscience Database [Internet] 2013. Landes Bioscience.
45. Lee TJ, Kim EJ, Kim S, Jung EM, Park JW, Jeong SH, et al. Caspase-dependent and caspase-independent apoptosis induced by evodiamine in human leukemic U937 cells. Mol Cancer Ther 2006;5:2398-407.
46. Yee KS, Wilkinson S, James J, Ryan KM, Vousden KH. PUMA-and Bax-induced autophagy contributes to apoptosis. Cell Death Differ 2009;16:1135-45.